



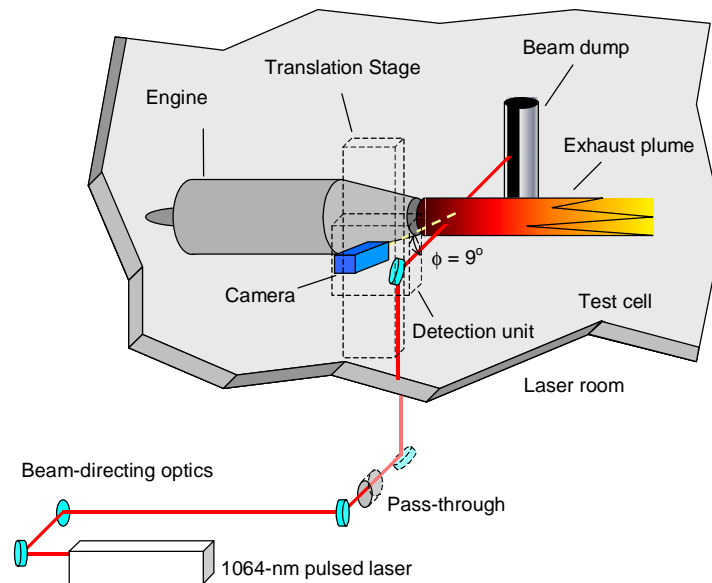
AIAA 2002-0828

Laser Induced Incandescence for Soot Concentration Measurements in Turbine Engine Exhausts

T. P. Jenkins, J. L. Bartholomew, and P. A. DeBarber
MetroLaser, Inc., Irvine, CA

P. Yang and J. M. Seitzman
Georgia Institute of Technology, Atlanta, GA

R. P. Howard
Sverdrup Technology, Inc., AEDC, TN



40th Aerospace Sciences Meeting & Exhibit
14–17 January 2002
Reno, Nevada

For permission to copy or to republish, contact the copyright owner named on the first page.
For AIAA-held copyright, write to AIAA Permissions Department,
1801 Alexander Bell Drive, Suite 500, Reston, VA, 20191-4344.

LASER INDUCED INCANDESCENCE FOR SOOT CONCENTRATION MEASUREMENTS IN TURBINE ENGINE EXHAUSTS

T. P. Jenkins*, J. L. Bartholomew[†] and P. A. DeBarber[‡]
MetroLaser, Inc., Irvine, CA

P. Yang[§] and J. M. Seitzman**
Georgia Institute of Technology, Atlanta, GA

R. P. Howard^{††}
Sverdrup Technology, Inc., AEDC, TN

Corresponding author: tjenkins@metrolaserinc.com

40th AIAA Aerospace Sciences Meeting and Exhibit January 14-17, 2002, Reno, NV

Abstract

To address the need for monitoring soot emanating from aircraft engines, a measurement system employing laser-induced incandescence (LII) has been developed and was successfully tested. The instrument instantaneously images up to a 1-m chord of an exhaust plume with a spatial resolution of 5.1 cm, and is capable of providing measurements of soot concentration down to 0.02 mg/m³. The system is completely non-intrusive and thus can be used to complement extractive sampling methods. Our efforts show how the LII method has matured to a level where it is ready for the harsh environment of an engine test cell. This paper describes the design and implementation of an LII system for soot concentration measurements in a full-scale, ground-based engine test, and presents results from such a test.

Introduction

Soot produced by aircraft engines has important military and civilian implications that warrant improved methods of measuring soot emissions during engine tests. The presence of soot in aircraft exhausts can contribute to an aircraft's infrared signature, making detection by enemy forces easier. Soot produced in flight by passenger aircraft may contribute to global warming¹, and near ground soot exhausts can cause health problems associated with small particles.² Current methods for measuring properties of soot in aircraft exhausts involve extractive sampling. Not hampered by spatial constraints of probe hardware and relatively slow response times of sampling lines, laser induced incandescence (LII) can provide real- or near real-time spatial profile measurements of soot mass

concentration with good temporal resolution. Important advantages to the turbine test community include significantly reduced test time for cross-sectional characterization of soot mass emissions and the ability to quickly track variations in soot mass for on-line monitoring during test programs.

LII has emerged as an attractive method for spatially resolved real-time soot concentration measurements in practical devices. The method was first explored by Eckbreth³, and involves heating soot particles using a laser to temperatures high enough that they incandesce. In a well-designed implementation, the incandescence intensity is nearly proportional to soot volume concentration. Recent efforts have demonstrated LII methods being applied to soot investigations of aircraft^{4,5} and automobile⁶ engines. The successes of these studies in jet engine testing applications have been limited. For example, susceptibility to the harsh conditions of an aircraft engine test has prevented quantitative LII data from being obtained non-intrusively⁴. However, the compromise of using an extractive sample cell for LII makes the method subject to the same errors associated with any extractive sampling technique. Our approach incorporates a rugged design and creative engineering to develop an *in-situ* LII measurement system for soot concentration profiles in aircraft engines. This system has been proven to be reliable and well suited for measurements in an engine test cell. Here we introduce the system, and present results from an engine test that demonstrates its success.

Experiment

The LII system consists of three subsystems: a Nd:YAG laser, a detection unit, and a computer control unit. The detection unit is located in the engine test section. The laser and computer control unit are located in rooms adjacent to the test section.

Fig. 1 shows the geometry of the measurement system. The exhaust plume is shown in cross section. The detection unit consists of a platform onto which is mounted a beam-steering mirror, an ICCD camera, and a

* Senior Scientist, AIAA member

[†] Scientist

[‡] Dir. Of Tech. Development, Senior Member

[§] PhD student, AIAA student member

** Assoc. Professor, AIAA Senior Member

^{††} Principle Investigator, AIAA Senior Member

Copyright © 2002 by MetroLaser, Inc.; Published by the American Institute of Aeronautics and Astronautics, Inc. with permission.

lens. To enable the measurement volume to be traversed vertically across the plume, the detection unit is mounted to a motorized translation stage. The beam from the 10-Hz pulsed 1064-nm Nd:YAG laser is directed horizontally through the plume. The resulting LII signal is captured by the camera in a near-backscatter configuration by having the lens axis tilted 9 degrees with respect to the laser beam axis. This arrangement allows the beam along the entire width of the plume, about 0.5 m, to be captured in one image frame.

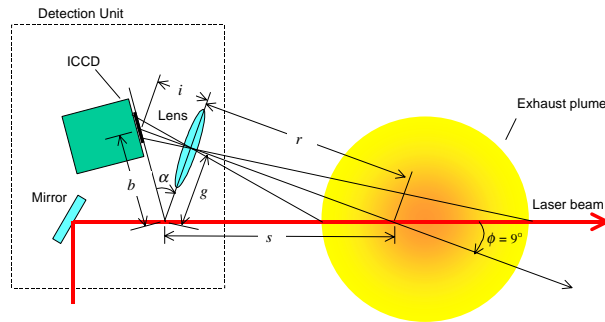


Fig. 1. LII system arrangement, showing the Scheimpflug geometry, for measuring soot concentration in aircraft engine exhausts.

For calibrating the LII system, a “soot generator” was developed that produces a steady stream of simulated soot aerosol⁷ at a known mass concentration. Fig. 2 depicts the soot generator, which operates as follows. A solution of carbon black in water is placed in a humidifier that atomizes the liquid into small droplets. A continuous flow of air passes through the humidifier, bringing the droplets through a heated tube where they are dried, producing an aerosol of carbon particles suspended in air and water vapor. The aerosol exits from a straight tube 16 mm in diameter. The mass concentration of the aerosol is accurately determined from the concentration of carbon in the solution, the airflow rate, and the loss rate of solution. Particle size distributions of the droplets from the atomizer have been obtained using a phase Doppler particle analyzer (PDPA), and reveal that the mean droplet diameter is about 20 μm . At a soot mass concentration of 1.0 mg/m^3 , assuming that all of the carbon contained in a single droplet forms into a particle when the water evaporates, the carbon particles should have a mean diameter of about 500 nm. Images taken with a scanning electron microscope of samples from the soot generator confirm that particles are near this size. Different particle sizes can be obtained by changing the carbon concentration in the solution, which determines the mass of carbon contained in a droplet and hence the particle size.

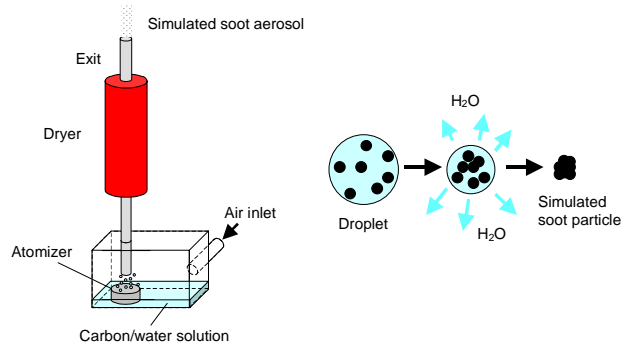


Fig. 2. Soot generator. Droplets produced by the atomizer are evaporated, leaving behind particles of carbon black that resemble soot.

Initial evaluation and calibration measurements were obtained in a laboratory setting using the arrangement depicted in Fig. 3 in which measurements were made at the exit of the soot generator. These measurements enabled optimization of intensifier gain setting, timing, optical filtering, and beam trap design.

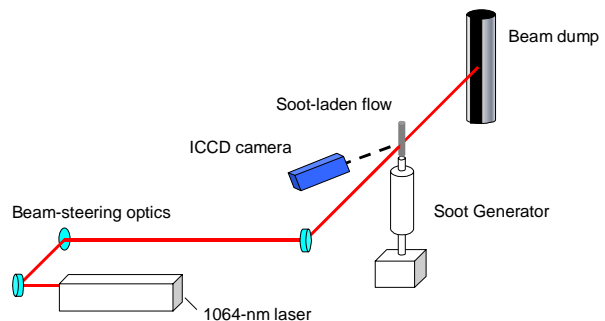


Fig. 3. Arrangement used for calibrating the LII system with the soot generator.

After optimizing in the laboratory, the system was moved to an engine test cell at the Arnold Engineering Development Center (AEDC). Fig. 4 depicts the arrangement of the system mounted in the AEDC test cell. The laser is mounted in an adjacent room to protect it from the vibration and other harsh conditions of the test cell, and the beam is passed through a hole between the two rooms. A rugged enclosure protects the components in the detection unit from dust, oil spray, and wind blasts that are present during engine tests. The detection unit was mounted to a heavy-duty motorized translation stage, which itself was mounted to the wall of the test cell.

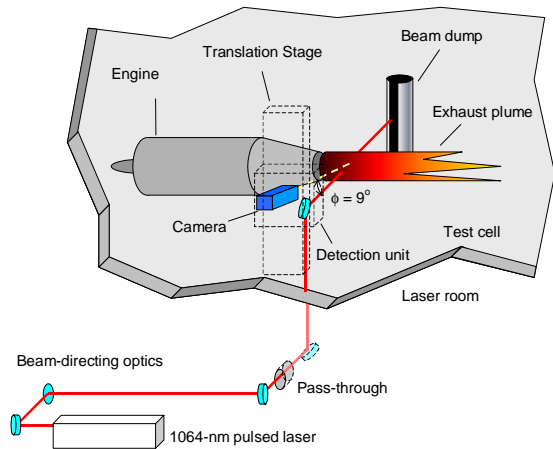


Fig. 4. LII system mounted in an engine test cell for measuring soot concentration in exhausts.

For the type of testing being done during these measurements, the engine was operated continuously for up to several hours. Special care had to be taken to ensure rigid mounting of all optics, since conventional adjustment screws tended to vibrate out of position during extended periods of testing. Success was achieved by using locking screws on all optical adjustments.

Fig. 5 shows the major electronic components of the system. Pulses produced by a pulse generator were used for triggering the laser. A second pulse generator that was slaved to the first was used for controlling the camera timing. The second pulse generator allowed a variable delay to be applied to the camera gate pulse, so that the timing of the camera gate could be accurately controlled with respect to the laser pulse. A computer located in the laser room controlled the pulse generators, laser, camera, and stage, and was also used for storage of the images from the camera. The computer was remotely operated by personnel located about 100 feet away in the test facility control room. Typical camera gate widths (exposure times) were 50 ns, and the delay after the laser pulse before the start of the camera gate was typically 10 ns.

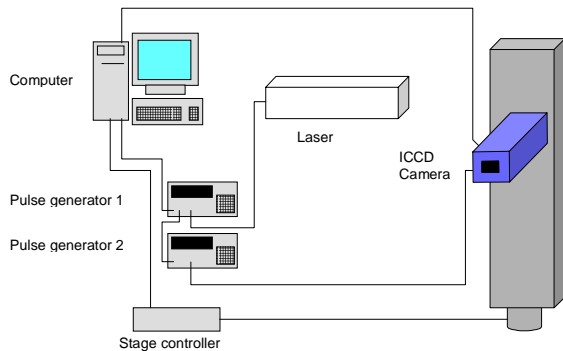


Fig. 5. Electronic components of the LII system

Results

Images obtained with our LII system are distorted due to the oblique imaging geometry shown in Fig. 1 and need to be corrected to reveal proper spatial relationships in the data. The condition whereby an object viewed at an oblique angle is brought into focus by tilting the image plane is known as the Scheimpflug⁸ condition. Referring to Fig. 1, the angle between the lens plane and the image plane, α , is given by⁹

$$\alpha = \arctan \frac{1}{\frac{g}{f} - \tan \phi}, \quad (1)$$

where g is the distance from the intersection of the image and object planes to the lens axis, (see Fig. 1), f is the focal length of the lens, and ϕ is the angle between the lens axis and the laser beam axis. The magnitude of this angle was selected to correspond to the lowest f-number lens that was readily available, resulting in $\phi = 9$ degrees, $f = 150$ mm, and $g = 325$ mm, leading to $\alpha = 26$ degrees. A relationship between the coordinate of the pixel, b , and the coordinate along the laser beam, s , (see Fig. 1) can be obtained by combining the lensmaker's formula, $1/i + 1/r = 1/f$, with Eqn. 1, resulting in

$$s = \frac{\sin \alpha}{\frac{\sin \alpha \cos \phi}{f} - \frac{\cos \phi}{b}}. \quad (2)$$

By applying Eqn. 2, the distorted image can be corrected by assigning the proper spatial coordinate to each pixel. Fig. 6 shows an uncorrected image taken of a 1-inch x 1-inch grid placed in the object plane, where the distortion is apparent. A 3/4-inch long screw is standing on the plane of the grid to help orient the viewer. The head of the screw is in focus since it is in the object plane, while the threads are out of focus. The entire grid is in focus since it is in the object plane, although the resolution decreases toward the far end of the grid. Fig. 7 shows the corrected image, in which it can be seen that the parallelism of the horizontal lines and the even spacing between vertical lines have been restored. The raw images of the data presented here were corrected in a similar fashion.

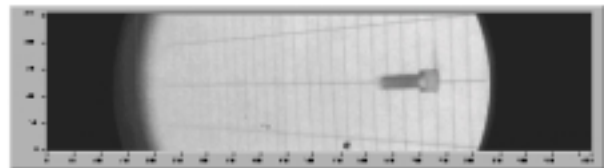


Fig. 6. Uncorrected image of a 1" x 1" grid placed in the measurement plane of the LII system.

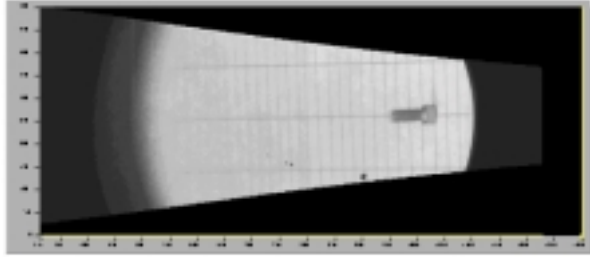


Fig. 7. The same image in Fig. 6 after correction.

Fig. 8 shows an example of a raw image of LII in the exhaust plume during an engine test, uncorrected for distortion. The LII appears as a thick line where the laser beam intersects the plume, as seen by the camera in the semi-backscatter arrangement discussed above. In this image, the exhaust flow is from bottom to top, and the laser beam propagation direction is from right to left. This image is an accumulation of 20 exposures from 20 pulses obtained over a period of 2 seconds. Spatial variations in intensity due to variations in soot concentration along the beam path can be seen. The spatial resolution along the beam is limited by the length of the beam segment viewed by the camera and is given by $d/\sin\phi$, where d is the diameter of the beam, about 8 mm, and ϕ is 9 degrees, giving a resolution of 5.1 cm. Because the angle between the viewing axis and the laser beam path, nominally 9 degrees, varies from one side of the LII image to the other, the path length through the soot that is imaged onto the camera will vary from pixel to pixel, changing by about 20 percent from one end of the illuminated section of the beam to the other. Consequently the measured intensity needs to be multiplied by a correction factor equal to the ratio of the calibration path length to the actual path length. This correction factor is easily calculated from the knowledge of the system geometry, and was applied to the raw data before presentation.

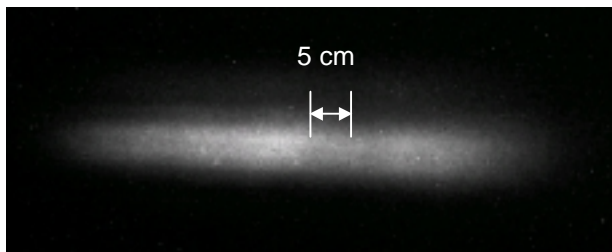


Fig. 8. Image of LII from soot in an aircraft engine exhaust plume. The laser propagates from right to left, and the exhaust flow direction is from bottom to top.

Data were obtained during engine tests over a period of about six hours. Besides obtaining images similar to Fig. 8, data in the form of a series of binned pixels were also obtained by hardware-binning the pixels in the vertical columns before reading out the data from the camera. The data from a given image thus was stored as vertically-summed LII intensities distributed across the plume.

These summed intensities were corrected for fact that due to the distortion a greater number of illuminated pixels would be summed on the side closest to the camera than on the far side. Note that the intensity measured by a given pixel is insensitive to the object distance because the decrease in intensity with $1/r^2$ cancels the increase in the area imaged by a pixel. Long durations of data collection were possible in which the data for one-second exposures were stored for a total of 3000 seconds, long enough to cover an entire mission of engine power settings. To quantify soot concentrations, the test data signal levels were normalized by a calibration signal obtained from a soot generator measurement at a “known” concentration of 1.0 mg/m^3 . However, it should be noted that a flow meter problem limited the accuracy of the calibration for the measurements reported herein. It is estimated that the uncertainty in the stated soot mass concentrations is on the order of 300 percent, but this was not quantified by measurement. This large uncertainty is not inherent to the technique. With a properly functioning flow meter the uncertainty in the measurements would be dominated by the uncertainty in the characteristic particle size. This translates to a systematic uncertainty in the LII signal of about 40 percent if no information about particle size is known, and may be lower with some knowledge of particle size. In any case, spatial and temporal relations among in the present data should be accurate.

Fig. 9 shows an example of the binned data in which soot mass concentration is plotted as a function of the transverse coordinate across the plume, s , and time, t . Each transverse profile represents one second of data, for a total of about 20 seconds in the figure. It can be noted that details of instantaneous soot distributions in the plume are revealed. An examination of the noise level indicates that concentrations down to 0.02 mg/m^3 can be detected. During this series of measurements, the throttle setting, indicated along the left side of Fig. 9, was rapidly adjusted from idle to maximum power. The trends observed in going from a lower to a higher power setting were consistent throughout the data. Fig. 10 shows data for an increase from idle to intermediate power, while Fig. 11 shows an example of going from high cruise to intermediate power. A momentary increase of soot can be seen in all such cases during the transition. Fig. 12 shows an example in which two kinds of power transitions can be observed: first low-to-high, then a few seconds later high-to-low.

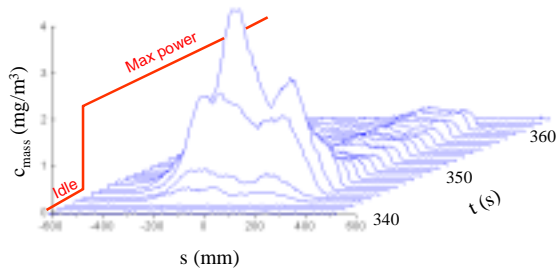


Fig. 9. Soot mass profiles in an engine exhaust for a transition from idle to maximum power.

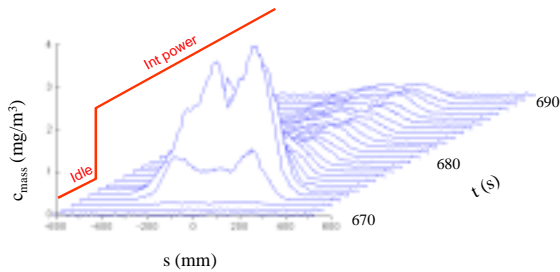


Fig. 10. Soot mass profiles in an engine exhaust for a transition from idle to intermediate power.

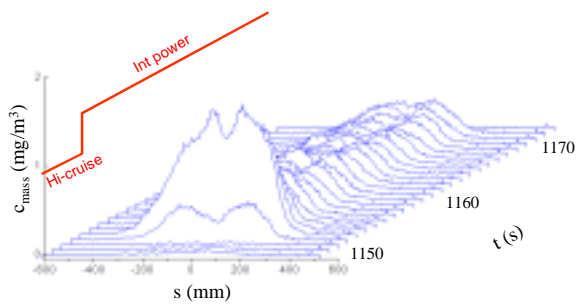


Fig. 11 Soot mass profiles in an engine exhaust for a transition from high cruise to intermediate power.

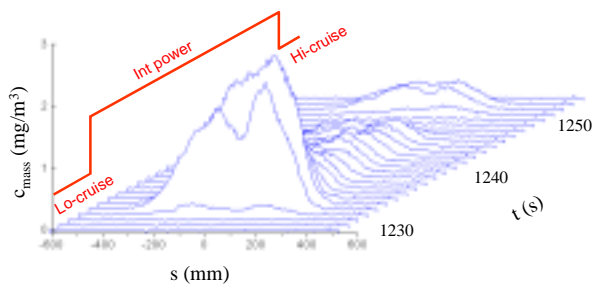


Fig. 12. Transverse profiles of soot concentration showing both low-to-high and high-to-low power changes.

By integrating the soot concentration profiles along the transverse coordinate, s , and dividing by a characteristic plume diameter of 0.5 m, an average soot concentration across the plume was obtained. Fig. 13 shows the integrated averages for an entire mission plotted as a function of time. During this experimental run the data

was continuously collected and stored for 46 minutes. The optics stayed aligned throughout this run, as was checked by noting that the position of the beam was the same on raw images taken before and after the run. The power settings for the mission appear at the top of the plot. Greater detail of this same data set is shown in an expanded region of the data in Fig. 14, where it can be seen that each low-to-high power transition is accompanied by a large momentary surge in soot concentration

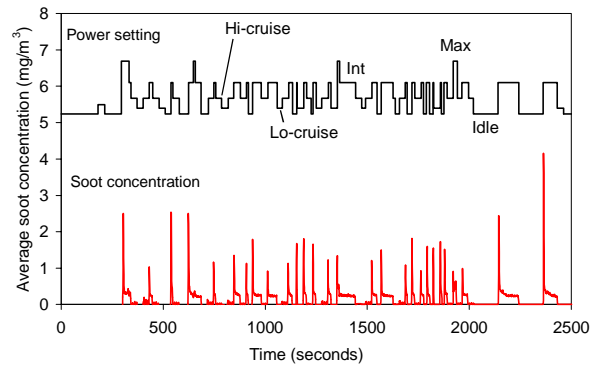


Fig. 13. Soot mass concentration averaged across the plume during an entire mission.

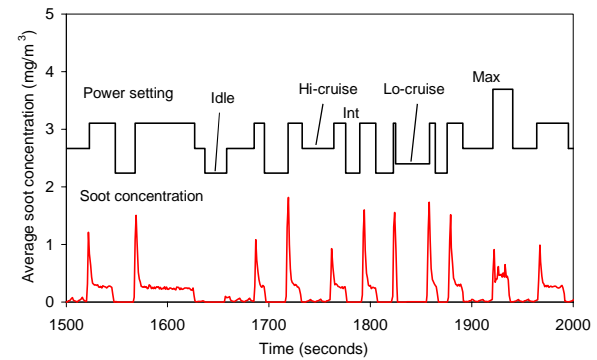


Fig. 14. Details of data for the entire-mission run of Fig. 13.

Discussion

In a typical application of LII, the detection optics are aligned at a right angle to the direction of the laser beam propagation. This arrangement produces the shortest path length through the beam, and hence the best spatial resolution. However, detection at right angles requires access to the measurement location from two sides. In an engine test cell environment, components of the measurement system must be able to stand up to severe vibration as well as aerodynamic forces. There are few locations within a typical test cell that are suitable for optical components to be mounted to during engine tests.

Thus, a measurement system that requires access from only one side has a distinct advantage, since it requires only one mounting location. By incorporating an oblique imaging geometry, our design has a single vantage point and enables spatially resolved LII measurements across the entire plume.

A significant amount of information can be obtained from the transverse profiles of Figures 9 through 12. Fig. 9 reveals that immediately after the throttle increase, the soot concentration jumps up to about 4 mg/m^3 , remains there for a few seconds, and then falls sharply to a steady value of about 0.3 mg/m^3 . This transient response to power changes is typical of what was observed in going from low to high power, as shown in Figures 10 and 11 for other transitions in the same direction. The bimodal and asymmetric character of the soot concentration profiles demonstrates important spatial profile information. In Fig. 12, soot concentration closely follows the changes in the engine power profile, both upward and downward. In all cases a local minimum in soot concentration can be seen in the middle of the plume during transitions.

Information gained from tests such as those shown in Figures 13 and 14 may help mission planners to evaluate possible contributions to plume signature for a given maneuver; some maneuvers can be observed to produce more soot than others. Also, because the presence of soot indicates inefficient combustion, the monitoring of surges in soot concentration during operation may help engine designers to optimize for efficiency.

Future work is planned on demonstrating velocity measurements in engine exhausts using particle vaporization velocimetry.¹⁰ This technique takes advantage of the vaporization of soot particles at high laser energies to produce a “hole” in the soot, which is convected downstream by the flow. The hole is imaged by scattering or LII using a laser sheet after a known time delay and the displacement yields the velocity.

Conclusions

An LII system for measuring soot concentrations in turbine engine exhausts has been developed, installed in an engine test cell, and successfully demonstrated. Spatially resolved, real-time, *in-situ* LII measurements were made in the exhaust of an aircraft engine during ground testing that compliments the capabilities of current measurement techniques. The rugged design of the system enabled it to operate well throughout a six-hour period of continuous engine testing, despite the harsh environment of the test cell. Initial tests showed that large variations in the overall soot mass concentration correlated with changes in engine power settings, especially when going from a lower to a higher power setting. Data such as these should be valuable to military

mission planners in reducing IR signatures as well as to engine designers for monitoring engine operation.

Acknowledgments

This effort was sponsored by a contract under the Arnold Engineering Development Center, Air Force Materiel Command, USAF.

REFERENCES

- ¹ J. Hansen, J. Sato, R. Ruedy, A. Lacis, and V. Oinas, “Global Warming in the Twenty-first Century: An Alternative Scenario”, *Proc. Natl. Acad. Sci.* **29**(18) pp. 9875-9880, 2000.
- ² Environmental Protection Agency website: <http://www.epa.gov/globalwarming/greenhouse/greenhouse6/part.html>, 2001.
- ³ A. C. Eckbreth, “Effects of Laser-Modulated Particulate Incandescence on Raman Scattering Diagnostics”, *Journal of Applied Physics* **48**, pp. 4473-4479, 1977.
- ⁴ K. Schafer, J. Heland, D. H. Lister, C. W. Wilson, *et al.*, “Nonintrusive Optical Measurements of Aircraft Engine Exhaust Emissions and Comparison with Standard Intrusive Techniques”, *Applied Optics* **39**(3), pp. 441-454, 2000.
- ⁵ M. G. Allen, B. L. Upschulte, D. M. Sonnenfroh, W. T. Rawlins, *et al.*, “Infrared Characterization of Particulate and Pollutant Emissions from Gas Turbine Combustors”, AIAA paper 2001-0789, 2001.
- ⁶ G. J. Smallwood, D. R. Snelling, O. L. Gulder, D. Clavel, *et al.*, “Transient Particulate Matter Measurements from the Exhaust of a Direct Injection Spark Ignition Automobile”, SAE paper 2001-01-3581, 2001.
- ⁷ R. T. Wainner and J. M. Seitzman, “Soot Measurements in a Simulated Engine Exhaust using Laser-Induced Incandescence,” *AIAA Journal* **37**(6), pp. 738-743, 1999.
- ⁸ A. K. Prasad and K. Jensen, Scheimpflug Stereocamera for Particle Image Velocimetry in Liquid Flows”, *Applied Optics* **34**(30), pp. 7092-7099, 1995.
- ⁹ S. Clausen and P. Astrup, “Oblique Laser-Sheet Visualization”, *Applied Optics* **34**(19), pp. 3800-3805, 1995.
- ¹⁰ P. Yang, J. M. Seitzman, and R. T. Wainner, “Particle Vaporization Velocimetry for Soot-Containing Flows”, AIAA paper 2000-0645, 2000.